

# Using Orbit Propagation to Probe the Thermospheric Dynamic Response to Geomagnetic Energy Input

Daniel A. Brandt, Aaron J. Ridley, Charles D. Bussy-Virat

University of Michigan Department of Climate and Space Sciences and Engineering



## Abstract

The neutral density of the thermosphere is highly responsive to changes in the space environment. Empirical atmospheric models, like NRLMSISE-00, poorly model the density response during geomagnetic storms, reducing the accuracy of orbital propagators, affecting estimates of the time and location of satellite reentry, and jeopardizing our ability to perform spacecraft collision avoidance. We demonstrate an observable density under-prediction during geomagnetic storms by NRLMSISE-00 in the lower thermosphere, and present a method for investigating thermospheric storm-time density behavior by rectifying this under-prediction using Two-line Element Sets (TLEs) and an orbital propagator, the Spacecraft Orbital Characterization Kit (SpOCK), to develop a calibration algorithm that reduces orbit error.

## Objective

- Perform orbit error minimization using three distinct methods to adjust satellite geometry factor and geomagnetic indices during periods of both high and low geomagnetic activity (assume free molecular flow)
- Describe trends in scale factors to the spacecraft geometry and geomagnetic indices to determine presence of periodic effects (solar rotation, rate of satellite nodal precession)
- Generalize the method to other spacecraft

## Introduction

The USAF stores orbital data in the form of TLEs via space-track.org. TLEs describe the average orbital state of an object within a usually 3-day fit span and include information corresponding to initial position and velocity vectors. These orbital data show increased decay rates during high geomagnetic activity (Figure 1) due to increased drag (Kim et al. 2006). Trying to reproduce TLE altitude profiles with orbital propagators like SpOCK (Bussy-Virat et al. 2018) that depend on NRLMSISE-00 show that empirical models underestimate the density during geomagnetic storms (Figure 2). This yields along-track bias in orbit propagation error (Figure 3). Since the density predictions SpOCK uses rely on modeled values for geomagnetic indices such as F10.7 and  $a_p$ , we reason empirical models handle them incorrectly during storms. We can adjust these geomagnetic inputs to NRLMSISE-00 to minimize orbit error, rather than *directly* calculating the density from TLEs and minimizing modeled densities to those from TLEs, as has been done previously (Doornbos et al. 2008, Storz et al. 2005).

6-hour Average Correlation of Dst and dSMA/dt: 2018-08-16 to 2018-09-05 (20 Satellites)

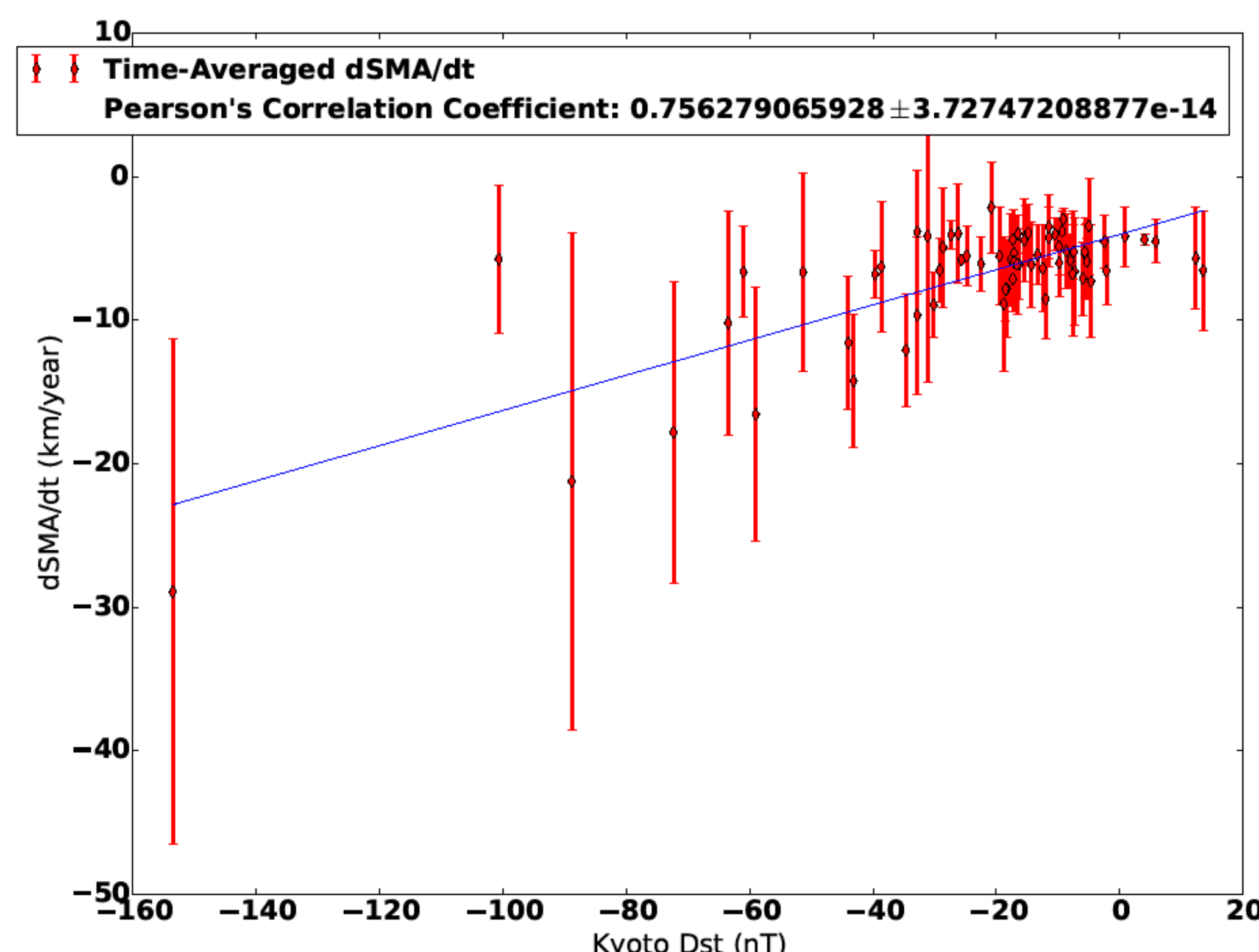


Figure 1: The correlation between descent rate of the FLOCK 2K satellites and Kyoto Dst, a geomagnetic index that serves as a proxy for the strength of geomagnetic activity.

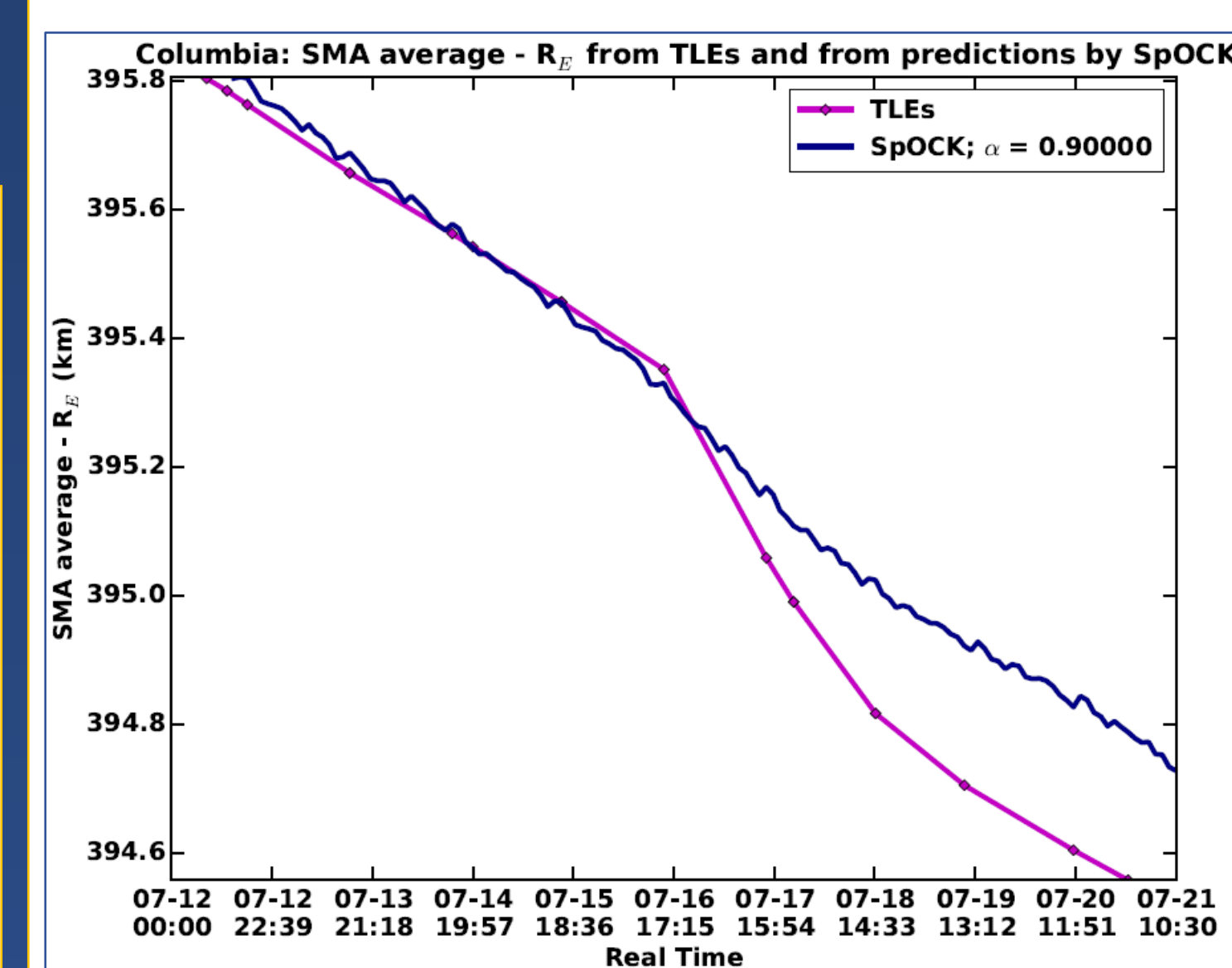


Figure 2: Altitudes recorded by TLEs for the QB50 CubeSat Columbia (magenta) and an erroneous reproduction by SpOCK relying on NRLMSISE-00 (blue), during a minor geomagnetic storm that began July 15, 2017.

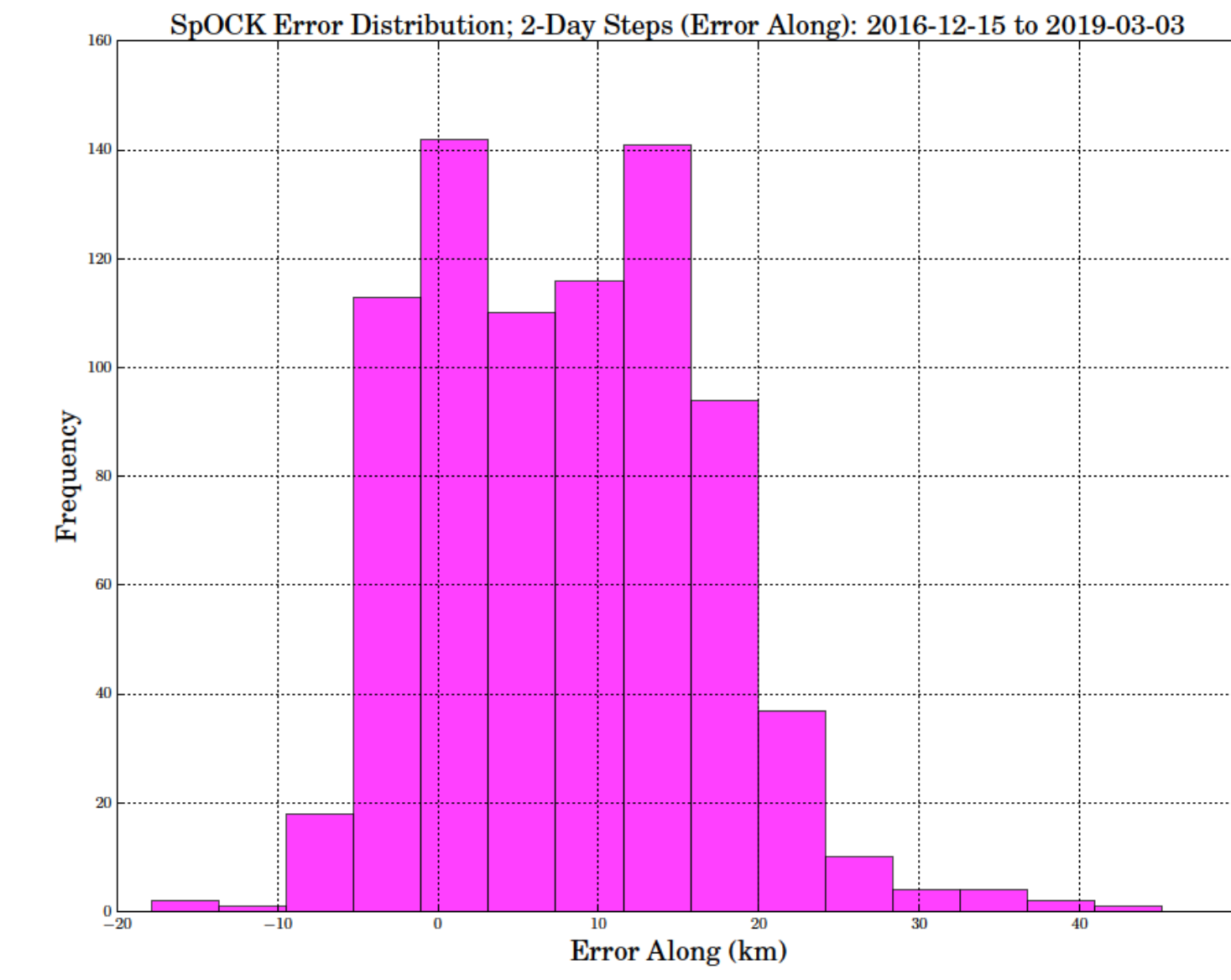


Figure 3: The distribution of along-track orbit error for the 8 satellites of the CYGNSS constellation over the majority of their orbit lifetimes. Positive bias in along-track orbit error implicates NRLMSISE-00 density underestimation.

## Methodology

We begin by using the accommodation coefficient to calculate a variable drag coefficient. We then minimize orbit error by segmenting a time period into small chunks, and running SpOCK along each chunk with a variable cross-sectional area until orbit error is minimized according to either RMS error between TLEs and SpOCK, the error of the last TLE and SpOCK altitudes, or the error in the total change in TLE and SpOCK altitudes (Figures 4 and 5).

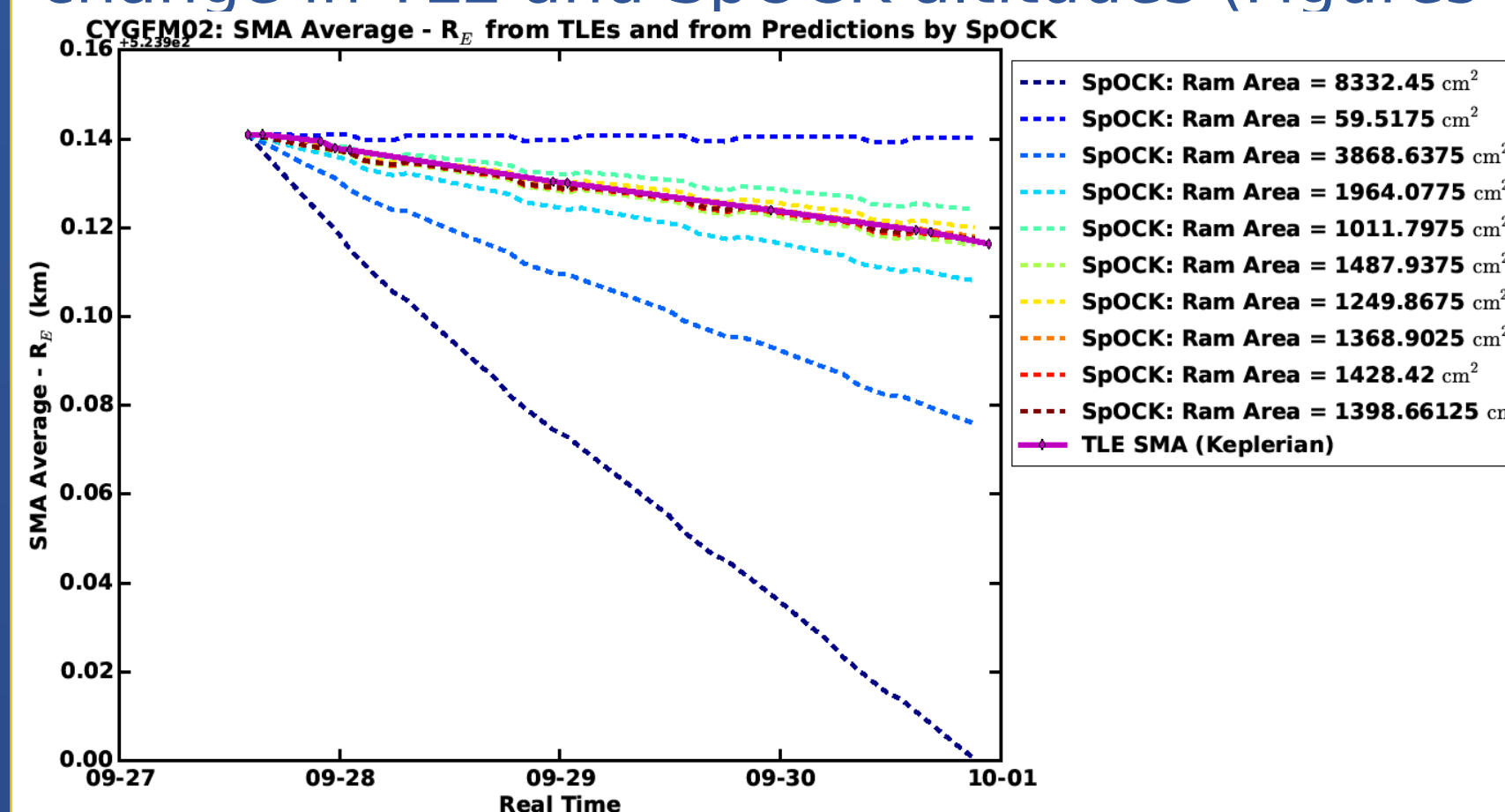


Figure 4: A completed run of the optimization algorithm for one time chunk in late September 2017 for the second CYGNSS spacecraft.

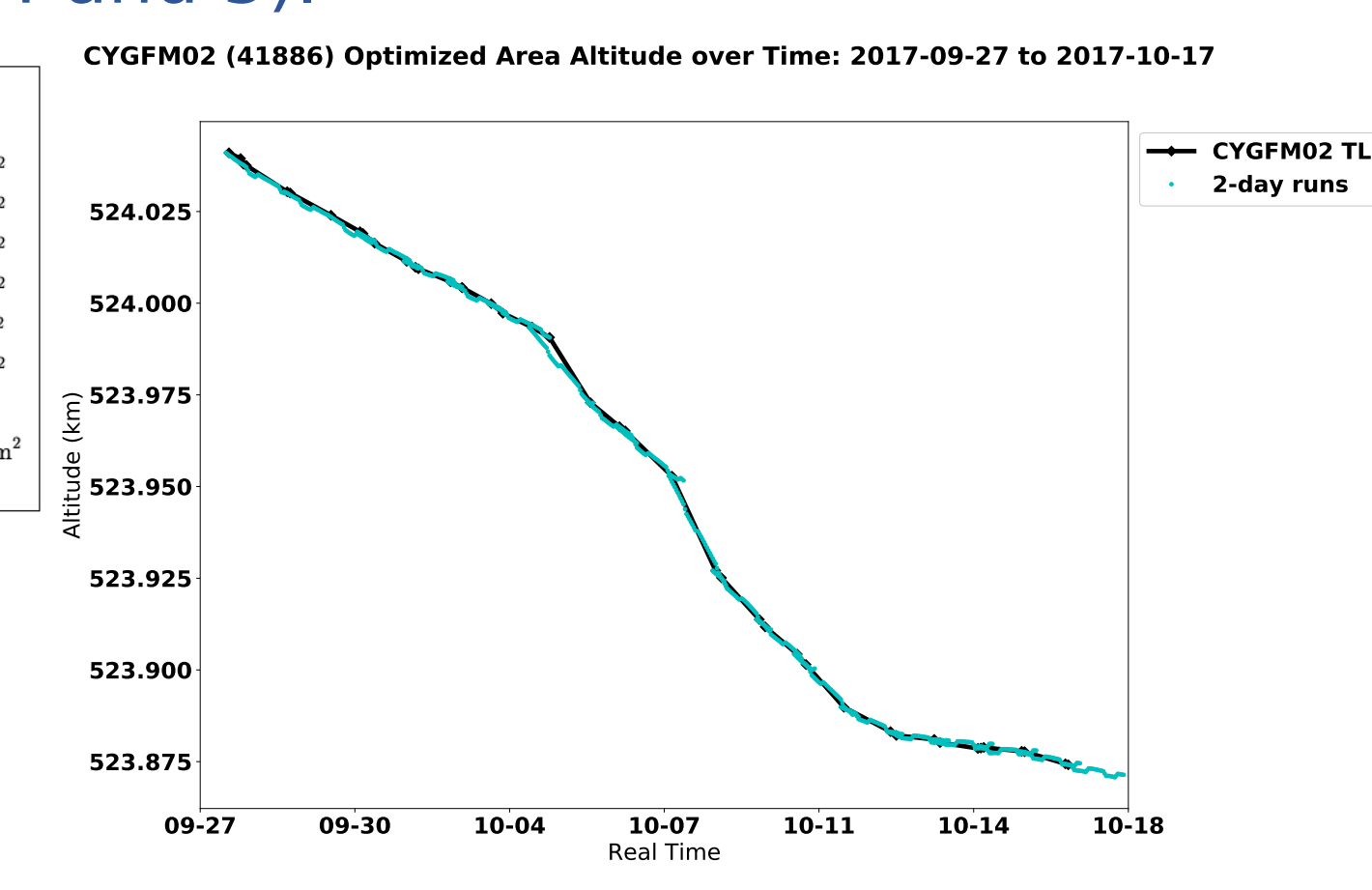


Figure 5: The corrected orbit resulting from adjustments to the cross-sectional area for the second CYGNSS spacecraft.

CYGM02 (41886) Optimized Area over Time: 2017-09-27 to 2017-10-17

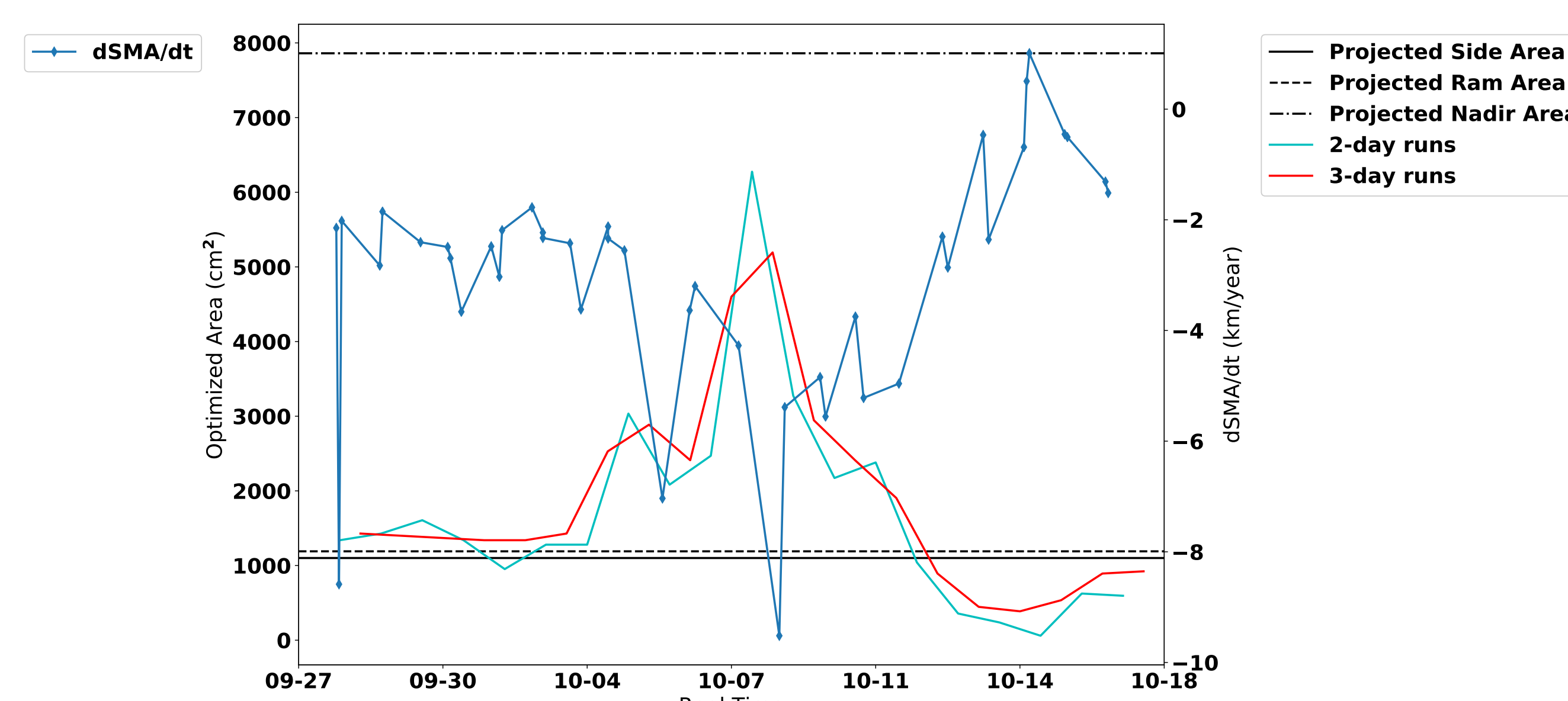


Figure 6: The behavior of the optimized cross-sectional area computed over both 2-day and 3-day intervals, over-plotted with the rate of orbital decay for the second CYGNSS spacecraft.

We then continue using a fixed area, varying F10.7 solar radio flux in quiet time and 3-hour  $a_p$  during storm-time, finally yielding **adjusted model densities**. These densities will be validated against accelerometer-derived densities from CHAMP, GRACE, and GOCE, **not** those derived from TLEs using B\*, which was designed specifically for use with SGP4 and introduces bias related to neglect of solar radiation pressure perturbations (Picone et al. 2005). Following validation, the adjusted model densities will be computed for various storm periods to better describe storm-time density behavior, and eventually used for trajectory prediction.

## Results

Three methods of orbit minimization were performed. The algorithm is proficient at minimizing orbit error to 3 orders of magnitude for the RMS method of orbit minimization and beyond 5 orders of magnitude for the Ending Error method and dSMA method (Figure 7). The behavior of optimized area computed for QB50 Atlantis and Columbia track closely to one another, suggesting orbital perturbations not solely attributable to changes in altitude (Figure 8).

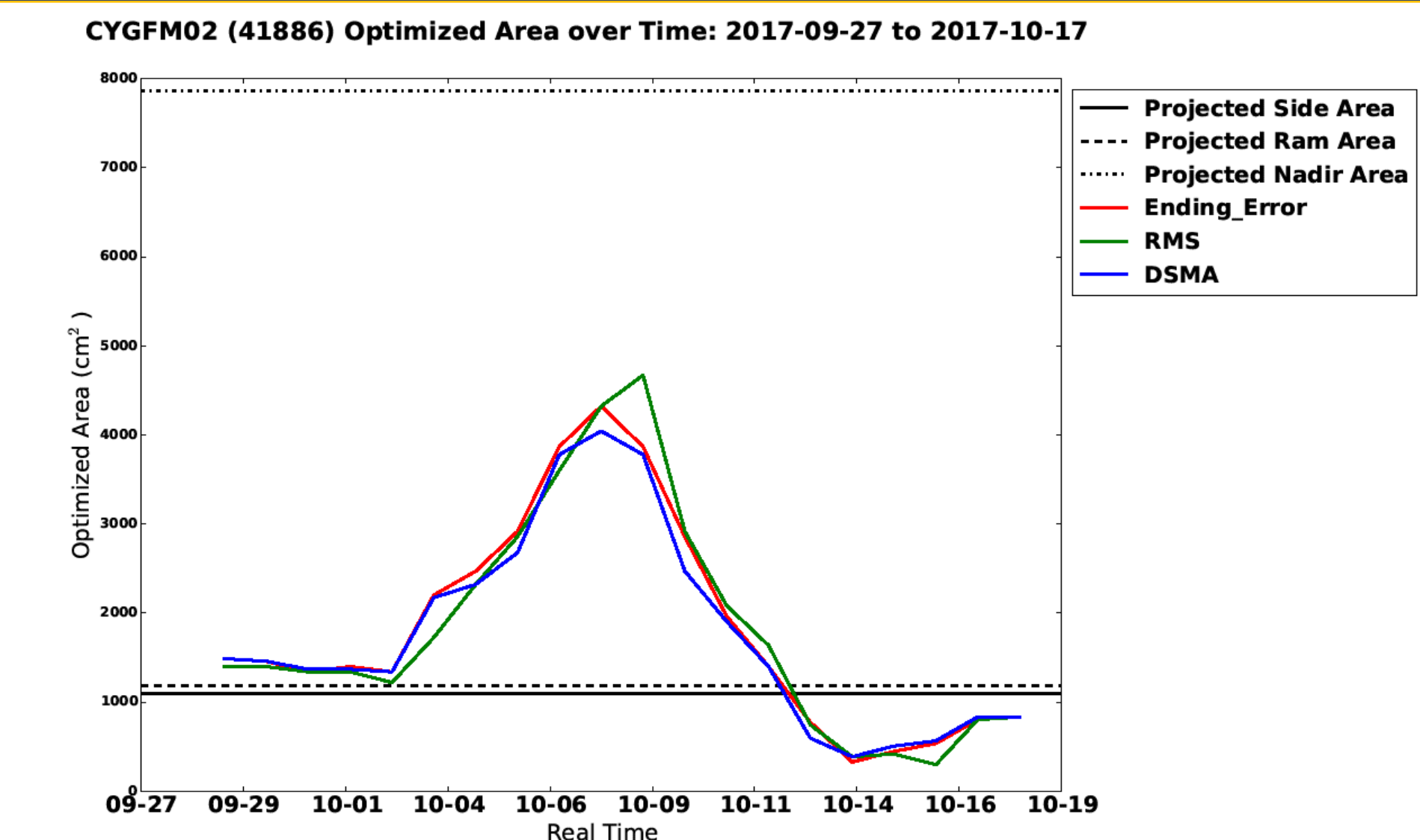


Figure 7: Optimized area results from each method for the second CYGNSS satellite.

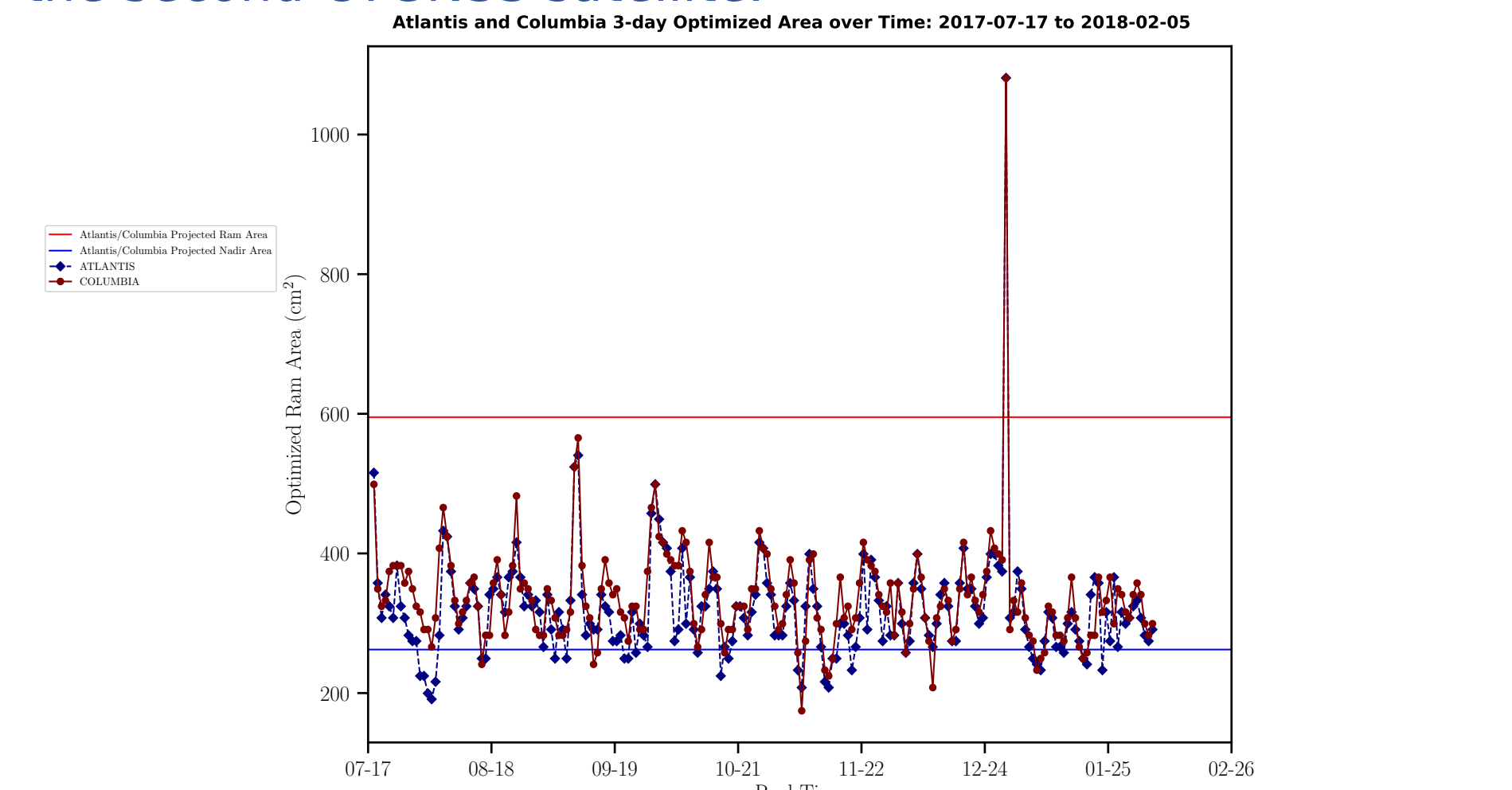


Figure 8: Optimized area over time for the UofM QB50 CubeSats Atlantis and Columbia.

## Conclusions and Future Work

The three orbit error minimization methods are mutually consistent and their use suggests geomagnetic effects as a necessary contributor to the variability of thermospheric dynamics enough to consistently affect orbits across multiple spacecraft. We intend to explore this using with orbital data from other satellites. We additionally aim to reveal whether or not these patterns persist exist for other density models (CIRA-72, DRM2013, JB2008, etc.) We will perform corollary analyses with F10.7 and  $a_p$ , and in completing the error optimization algorithm, validate the adjusted model densities before looking at various storms and performing orbit prediction.

## References

- Bussy-Virat, C. D., et al., The Spacecraft Orbital Characterization Kit and its Applications to the CYGNSS Mission, *2018 Space Flight Mechanics Meeting*, AIAA SciTech Forum, **AIAA 2018-1973**, 2018
- Doornbos, et al., Use of two-line element data for thermosphere neutral density model calibration, *Adv. Sp. Res.*, **41**, pp. 1115-1122, 2008.
- Kim, K.-H., et al., Atmospheric drag effects on the KOMPSAT-1 satellite during geomagnetic superstorms, *Earth Planets Space*, **58**, e25-e28, 2006.
- Picone, et al., Thermospheric densities derived from spacecraft orbits: Accurate processing of two-line elements sets, *J. Geophys. Res.*, **110**, A03301, 2005.
- Storz, M. F., et al., High accuracy satellite drag model (HASDM), *Adv. Sp. Res.*, **36**, 12, pp. 2497-2505, 2005.

## Contacts

Daniel A. Brandt - branddan@umich.edu  
 Aaron J. Ridley, PhD - ridley@umich.edu  
 Charles D. Bussy-Virat, PhD - cbv@umich.edu